ANTIOXIDANTS & REDOX SIGNALING
Volume 00, Number 00, 2014
© Mary Ann Liebert, Inc.
DOI: 10.1089/ars.2013.5589

FORUM ORIGINAL RESEARCH COMMUNICATION

Novel Lipophilic Probe for Detecting Near-Membrane Reactive Oxygen Species Responses and Its Application for Studies of Pancreatic Acinar Cells: Effects of Pyocyanin and L-Ornithine

Michael Chvanov,[1,2] Wei Huang,[2,3] Tao Jin,[2,3] Li Wen,[2,3] Jane Armstrong,[2] Vicky Elliot,[2] Ben Alston,[4] Alex Burdyga,[1] David N. Criddle,[1,2] Robert Sutton,[1,2] and Alexei V. Tepikin[1]

Abstract

Aims: The aim of this study was to develop a fluorescent reactive oxygen species (ROS) probe, which is preferentially localized in cellular membranes and displays a strong change in fluorescence upon oxidation. We also aimed to test the performance of this probe for detecting pathophysiologically relevant ROS responses in isolated cells. ***Results:*** We introduced a novel lipophilic ROS probe dihydrorhodamine B octadecyl ester (H_2RB-C_{18}). We then applied the new probe to characterize the ROS changes triggered by inducers of acute pancreatitis in pancreatic acinar cells. We resolved ROS changes produced by L-ornithine, L-arginine, cholecystokinin-8, acetylcholine, taurolithocholic acid 3-sulfate, palmitoleic acid ethyl ester, and the bacterial toxin pyocyanin. Particularly prominent ROS responses were induced by pyocyanin and L-ornithine. These ROS responses were accompanied by changes in cytosolic Ca^{2+}concentration ($[Ca^{2+}]_i$), mitochondrial membrane potential ($\Delta\Psi$), and NAD(P)H concentration. ***Innovation:*** The study describes a novel sensitive lipophilic ROS probe. The probe is particularly suitable for detecting ROS in near-membrane regions and therefore for reporting the ROS environment of plasma membrane channels and pumps. ***Conclusions:*** In our experimental conditions, the novel probe was more sensitive than 5-(and-6)-chloromethyl-2′,7′-dichlorodihydrofluorescein (CM-H_2DCF) and dihydrorhodamine123 (H_2R123) and allowed us to resolve ROS responses to secretagogues, pyocyanin, and L-ornithine. Changes in the fluorescence of the new probe were particularly prominent in the peripheral plasma membrane-associated regions. Our findings suggest that the new probe will be a useful tool in studies of the contribution of ROS to the pathophysiology of exocrine pancreas and other organs/tissues. *Antioxid. Redox Signal*. 00, 000–000.

Introduction

REACTIVE OXYGEN SPECIES (ROS) serve as signaling molecules but may also cause cell injury (24). Increased ROS levels are hallmarks of many pathological processes and conditions, including ischemia-reperfusion injury (7), inflammatory tissue damage and autoimmune reactions (30, 31, 45), aging (29), neurodegeneration (41), and cancer (66). Studies of ROS changes in live cells with the help of fluorescent probes are important avenues for determining the mechanisms of ROS production and ROS functions. Derivatives of fluorescein and rhodamine have been extensively used in such studies (16, 21, 35, 72). One of the challenges of monitoring the ROS and reactive nitrogen species production in live cells using fluorescent probes is the abundance of cytosolic antioxidants, such as glutathione and ascorbate (19,

[1]Department of Cellular and Molecular Physiology, Institute of Translational Medicine, University of Liverpool, Liverpool, United Kingdom.
[2]NIHR Liverpool Pancreas Biomedical Research Unit, Royal Liverpool University Hospital, Liverpool, United Kingdom.
[3]Sichuan Provincial Pancreatitis Center, West China Hospital, Sichuan University, Chengdu, People's Republic of China.
[4]CTL Department of Chemistry, University of Liverpool, Liverpool, United Kingdom.

Innovation

The study describes a novel lipophilic reactive oxygen species (ROS) probe, which performed better than popular small molecule probes for ROS measurements in primary isolated cells (pancreatic acinar cells). The probe was particularly effective for resolving near-membrane ROS responses and was used to reveal dynamic changes of ROS in response to inducers of acute pancreatitis (including novel effects of pyocyanin and L-ornithine).

32, 55). In this study, we aimed to introduce a fluorescent ROS probe, which is preferentially localized in cellular membranes. We hypothesized that such a probe could be more responsive to cellular ROS due to a decrease in competition from cytosolic antioxidants. We expected that this probe will preferentially detect ROS production in membranes or in near-membrane regions.

We selected pancreatic acinar cells to test the performance of the new ROS probe in resolving ROS responses triggered by inducers of acute pancreatitis (AP). One common property of the inducers of AP is that they trigger Ca^{2+} signals and prolonged Ca^{2+} elevation (Ca^{2+} overload), which is of paramount importance for the damage of acinar cells in conditions of AP (reviewed in Refs. 39, 50, 51, 62, 63). The relationship between Ca^{2+} signaling and ROS in acinar cells is complicated. Moderate mitochondrial ROS production seems to be important for the initiation of physiological Ca^{2+} signals and regulation of secretion in these cells (18). Ca^{2+} increase is required for taurolithocholic acid 3-sulfate (TLC-S)-induced ROS response (15). Oxidation inhibits the function of important Ca^{2+} influx channels (Orai channels) (12) and therefore could be protective against Ca^{2+} overload. Conversely, ROS inhibits plasma membrane Ca^{2+} ATPases and could therefore facilitate Ca^{2+} overload and cell damage (1). The amplitude and duration of ROS responses are probably critical in determining if these responses are going to be physiologically beneficial, protective, or damaging.

Mitochondria are important sources of ROS in many cell types, including pancreatic acinar cells (15, 18, 48). In our previous studies, we demonstrated the effect of inducers of pancreatitis on the mitochondria of these cells (15, 69, 70). Monitoring mitochondrial properties [*e.g.,* mitochondrial membrane potential ($\Delta\Psi$) and mitochondrial NAD(P)H concentration] and application of mitochondrial inhibitors could therefore help to reveal the mitochondrial component of ROS responses.

Although the generation of ROS after the induction of AP is firmly established in whole pancreas (the evidence for this is based on detecting lipid peroxidation products and protein carbonyls, on monitoring decreases in the antioxidant capacity, and on measurements employing spin-resonance spectroscopy (40, 68), sensing ROS in individual acinar cells upon physiological or pathological stimulation has been more challenging [reviewed in Ref. (20)].

Oxidative stress is considered to be a contributing factor in the pathogenesis of acute and chronic pancreatitis (reviewed in Refs. 14, 52, 56); however, the evidence for the significance of ROS in the initiation and development of pancreatitis is controversial. Strong depletion of glutathione in pancreatic tissue has been reported in a cerulein-induced model of AP and interpreted as a reflection of ROS contribution to the pathogenesis of this disease (44, 47); however, another study concluded that the depletion of glutathione is ''neither early nor critical'' for the development of cerulein-induced AP (27). Moreover, the usage of antioxidants has produced disappointing results in some clinical trials (5, 59). ROS have been shown to potentiate the release of cytochrome c from the mitochondria of pancreatic acinar cells and by this mechanism influence apoptosis in these cells (48). This is important since in conditions of AP, apoptosis is considered to be protective (28, 33, 57); reviewed in Ref. (6). Recently, it has been shown that ROS production in pancreatic acinar cells can reduce the pancreatic acinar cell necrosis and increase the apoptosis caused by bile acids, also suggesting a protective action of ROS (15). In this previous study, we used commercially available ROS probes and successfully resolved ROS responses induced by TLC-S (15), but we had difficulties in resolving and/or characterizing ROS changes upon application of other inducers of AP. This was an important motivation for the development of a new probe with improved sensitivity. The uncertainty of the role of ROS in the etiology of AP and the recent focus on ROS in acinar cells made this cell type (in conjunction with chemical inducers of AP) a promising platform for testing the new probe.

Results

H_2RB-C_{18}–lipophilic ROS-sensitive probe

Dihydrorhodamine B octadecyl ester (H_2RB-C_{18}) was prepared from the parent compound rhodamine B octadecyl ester (RB-C_{18}) by a standard sodium borohydride ($NaBH_4$) reduction procedure (10, 65) (Fig. 1A). Within seconds of the addition of $NaBH_4$, the dimethyl sulfoxide (DMSO) solution of RB-C_{18} lost its red color, indicating the conversion of RB-C_{18} into H_2RB-C_{18}. ROS, produced as a result of the Fenton reaction, oxidized H_2RB-C_{18} back into RB-C_{18} (this is revealed by the increase of fluorescence). ROS-induced oxidation of dihydrorhodamine123 (H_2R123) showed a similar response in a cell-free solution, confirming that H_2RB-C_{18} is a ROS-sensitive probe (Fig. 1A, right panel). The new probe was not sensitive to hydrogen peroxide (H_2O_2) *per se* (Fig. 1A and Supplementary Fig. S1A; Supplementary Data are available online at www.liebertpub.com/ars), but in the presence of Co^{2+} or Fe^{2+}, the addition of H_2O_2 resulted in the increase of fluorescence; in such cell-free conditions, 10 μM H_2O_2 produced clearly resolvable responses (Supplementary Fig. S1B, C). The fluorescence of H_2RB-C_{18} did not increase upon the addition of KO_2 (up to 1 m*M*, data not shown). However, the fluorescence of the probe moderately increased upon the addition of 4 mU/ml xanthine oxidase in the presence of acetaldehyde, and this increase was suppressed by 1.5 kU/ml superoxide dismutase (Supplementary Fig. S1D). It should be, however, noted that the response to xanthine oxidase and acetaldehyde was not observed in the presence of 1 m*M* EDTA (Supplementary Fig. S1D), suggesting that the Fenton reaction (*i.e.,* probably hydroxyl radical) and not the superoxide radical is responsible for the observed fluorescence changes (see Supplementary Fig. S2 for considerations regarding nomenclature and the relevant reactions). With regard to its relative sensitivity to H_2O_2, superoxide, and hydroxyl radicals, the new probe (H_2RB-C_{18}) in a cell-free system behaves similar to CM-H_2DCF and H_2R123 (38, 71).

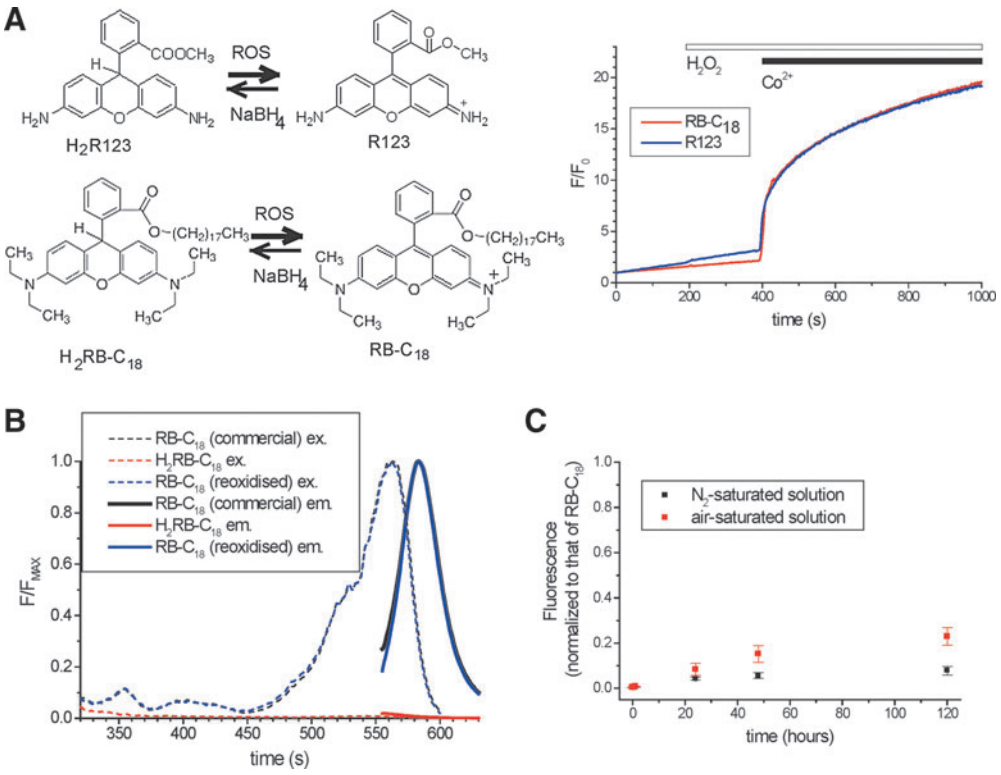

FIG. 1. Fluorescence responses, spectra, and stability of H_2RB-C_{18}. **(A)** *Left panel* illustrates the reduction of R123 and RB-C_{18} into ROS probes by $NaBH_4$ and oxidation back into fluorophores. *Right panel* shows the normalized fluorescence changes of the probes in a cell-free H_2O_2-containing solution upon addition of 10 μM Co^{2+} (*i.e.,* activation of the Fenton reaction); both probes strongly increase fluorescence upon oxidation. **(B)** Shows excitation (*dashed lines*) and emission (solid lines) fluorescence spectra of commercial RB-C_{18} (*black traces*), H_2RB-C_{18} was obtained by the reduction of commercial RB-C_{18} (*red traces*), and RB-C_{18} was obtained from reoxygenation of H_2RB-C_{18} in the presence of H_2O_2 and Co^{2+} (*blue traces*) in a cell-free solution. The spectra were normalized by the maximal values of excitation and emission recorded from the cuvette with RB-C_{18}-containing solution. Emission spectra were recorded with excitation set at 540 nm and excitation spectra were recorded at emission set at 620 nm. **(C)** Illustrates the stability of the probe in cell-free solutions. Measurements were conducted in the solution maintained in contact with air (*red dots*) and in the solution that was bubbled with nitrogen for 30 min and after that maintained in hermetically closed cuvettes (*black dots*). Maximal fluorescence of the oxidized probe corresponds to 1. The measurements show that less than 25% of H_2RB-C_{18} becomes oxidized during 120 h of exposure to atmospheric oxygen. H_2O_2, hydrogen peroxide; H_2RB-C_{18}, dihydrorhodamine B octadecyl ester; $NaBH_4$, sodium borohydride; RB-C_{18}, rhodamine B octadecyl ester; ROS, reactive oxygen species.

Importantly, the fluorescence of H_2RB-C_{18} in a cell-free system was not changed by the addition of substances that caused significant fluorescence changes in cells loaded with the probe: 500 μM TLC-S, 20 mM L-ornithine, or 50 μM pyocyanin (data not shown).

The excitation and emission fluorescence spectra of RB-C_{18} and H_2RB-C_{18} are shown in Figure 1B. The spectra of the commercial RB-C_{18} (purchased from Sigma-Aldrich and used to produce H_2RB-C_{18} in our experiments) largely overlap with the spectra of the product of oxidation of H_2RB-C_{18} (Fig. 1B). H_2RB-C_{18} is reasonably stable and can be used for a few hours after formation by $NaBH_4$ reduction; the stability of H_2RB-C_{18} in deoxygenated solution and in solution exposed to atmospheric oxygen is illustrated in Figure 1C.

Fluorescence of the cells loaded with the parent (oxidized) compound RB-C_{18} and with rhodamine B (RB: the same fluorophore but without the lipophilic tail) is shown in Figure 2A and B (see also Supplementary Fig. S3 for RB-C_{18} fluorescence distribution in an acinar cell cluster). Local photobleaching of RB-C_{18} by UV light leads to a much slower recovery of fluorescence than the recovery following the local photobleaching of RB (Fig. 2A, B). The slow diffusion of RB-C_{18} can be explained by the lipophilic nature of this compound. This property is probably responsible for the increased sensitivity of the new probe in the cellular environment (see next section).

H_2RB-C_{18} is a highly efficient probe for detecting cellular ROS responses

Using 5-(and-6)-chloromethyl-2′,7′-dichlorodihydrofluorescein diacetate [CM-H_2DCF(DA)], we have recently reported ROS responses induced by the bile acid TLC-S in pancreatic acinar cells (15). The new probe H_2RB-C_{18}, loaded into acinar cells, also produced clearly resolvable response to 500 μM TLC-S (Fig. 2C). Furthermore, the amplitude of this response was considerably larger than that recorded with CM-H_2DCF [see Ref. (15)], suggesting that H_2RB-C_{18} is a more sensitive indicator. In unstimulated cells, the fluorescence of H_2RB-C_{18} was nonuniform with a stronger peripheral (plasma membrane) component and weaker fluorescence in the central areas of the cell. The preferential

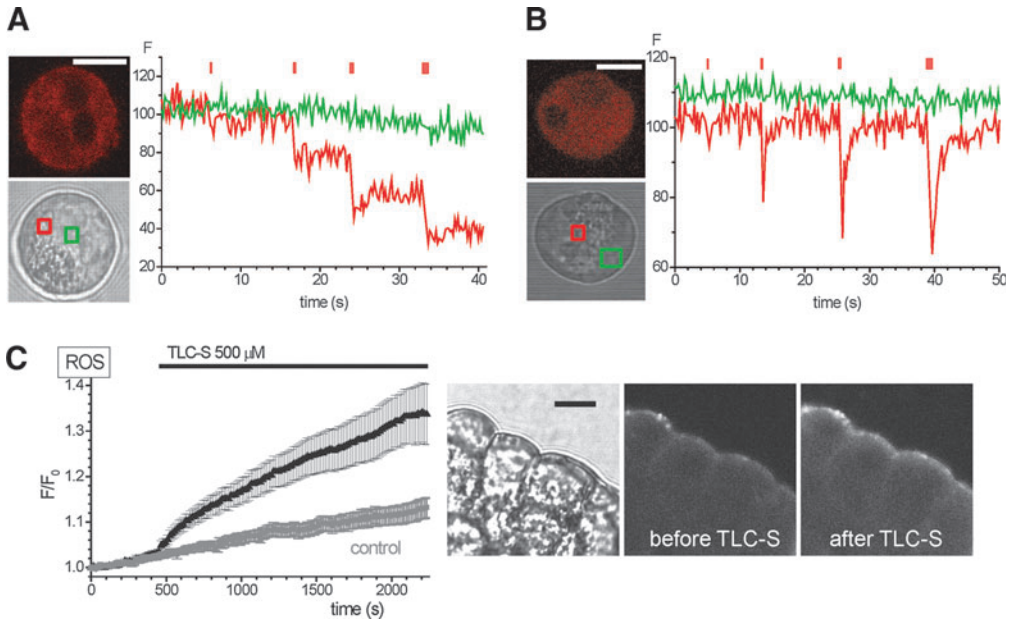

FIG. 2. $H_2RB\text{-}C_{18}$ is a highly sensitive lipophilic ROS probe. (A) Distribution of cell staining with $RB\text{-}C_{18}$ and regional photobleaching of the probe with pulses of UV light (351 and 365 nm laser lines). In **(A)** and **(B),** the *red trace* represents fluorescence changes recorded from the bleached area (*red rectangle*) and the *green trace* shows fluorescence changes in the region outside the bleached area (*green rectangle*). Periods of photobleaching are indicated by red bars above the traces. 543 nm laser line was used to continuously excite $RB\text{-}C_{18}$ fluorescence, and the emitted light was collected at >565 nm. Scale bars on the fluorescence confocal images correspond to 10 μm. The traces are representative of 11 similar experiments. **(B)** Cell staining with RB and the regional photobleaching of the probe. Fluorescence of the probe was excited by 543 nm laser line and recorded at >565 nm. Scale bars on the fluorescence confocal images correspond to 10 μm. The traces are representative of seven similar experiments. **(C)** ROS response induced by TLC-S in cells loaded with $H_2RB\text{-}C_{18}$. *Left panel* shows the average time course of the TLC-S response (*black*, $n=13$) *versus* control unstimulated cells (*gray*, $n=22$). The traces represent the averaged normalized fluorescence with corresponding SEM error bars. The fluorescence of TLC-S-treated cells became statistically different from that recorded from control cells after 45 s of stimulation. The *right panel* shows a representative fluorescence image of cells before and after stimulation with TLC-S. Scale bar corresponds to 10 μm. TLC-S, taurolithocholic acid 3-sulfate.

peripheral localization of fluorescence was also observed after stimulation of $H_2RB\text{-}C_{18}$-loaded cells with TLC-S (Fig. 2C).

Increased $H_2RB\text{-}C_{18}$ fluorescence was also detected in acinar cells stimulated by acetylcholine (ACh) (Fig. 3A) and in cells treated with palmitoleic acid ethyl ester (POAEE) (Fig. 3B). These experiments further confirm the usability of the new probe for ROS measurements in acinar cells. We also tested the effect of mitochondrial inhibitors on ROS production in unstimulated acinar cells and observed that the treatment with rotenone plus antimycin showed a tendency to reduce the rate of the basal rise of fluorescence (Fig. 3C); however, the basal rise of fluorescence was slow, the difference was not statistically significant, and this phenomenon was not investigated further.

The increased sensitivity of $H_2RB\text{-}C_{18}$ allowed us to detect the ROS changes induced by 10 n*M* cholecystokinin (CCK), which were not resolvable with CM-H_2DCF or H_2R123 (Fig. 4A–C). The high sensitivity of $H_2RB\text{-}C_{18}$ for detection of ROS changes was also obvious from experiments with L-ornithine; $H_2RB\text{-}C_{18}$ showed clearly resolvable responses to the application of this amino acid (Fig. 4D; see also Fig. 6D), while the changes of fluorescence of CM-H_2DCF and H_2R123 were much less pronounced (Fig. 4E, F). The strong response to L-ornithine recorded in cells loaded with $H_2RB\text{-}C_{18}$ was almost completely eliminated by an antioxidant dihydrolipoic acid (compare black and green traces in Fig. 4G) confirming that the $H_2RB\text{-}C_{18}$ response to L-ornithine develops as the result of ROS generation. Notably, cells loaded with $H_2RB\text{-}C_{18}$ did not display obvious indications of cellular damage (no blebbing and no vacuolization). Basal oxygen consumption rate (OCR) and the rates in the presence of Oligomycin and FCCP were also unchanged (Supplementary Fig. S4). We concluded from these data that $H_2RB\text{-}C_{18}$ is well tolerated by the acinar cells and, under our experimental conditions, provides improved sensitivity for the detection of cellular ROS changes. We therefore decided to employ this new probe to characterize the effects of the putative ROS-producing damaging agents (pyocyanin and L-ornithine) on pancreatic acinar cells.

Pyocyanin-induced ROS responses measured with $H_2RB\text{-}C_{18}$

Pseudomonas aeruginosa, which has been shown to infect the pancreas in AP, cystic fibrosis, pancreatic transplantation, and endoscopic retrograde cholangiopancreatography receiving patients (9, 13, 42, 67), can produce copious amounts of pyocyanin (17, 73). Local concentrations of pyocyanin can reach 100 μM or even higher (17, 73). Unlike the action of

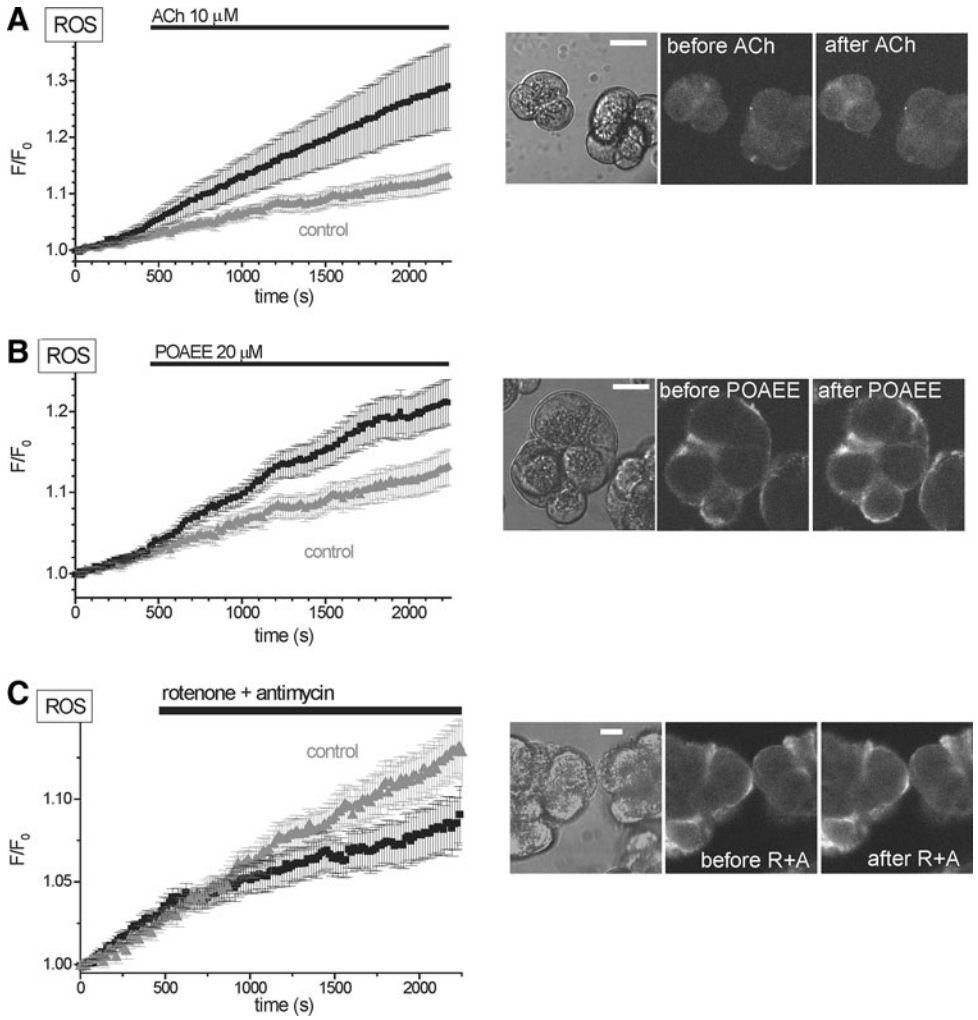

FIG. 3. ROS responses to ACh, POAEE, and the inhibition of mitochondrial transport chain. In all the experiments illustrated in this figure, the cells were loaded with H_2RB-C_{18}. **(A)** *Left panel* shows the average time course with corresponding SEM, error bars of ROS responses to 10 μM ACh ($n=16$) *versus* control unstimulated cells (*gray*, $n=22$). *Right panel* shows transmitted image (nonconfocal, scale bar corresponds to 10 μm) and confocal fluorescence images of pancreatic acinar cells before ($t=0$ s) and after ($t=2250$ s) stimulation with 10 μM ACh. **(B)** *Left panel* shows the average time course with corresponding SEM error bars of ROS responses to 20 μM POAEE ($n=12$) *versus* control unstimulated cells (*gray*, $n=22$). *Right panel* shows transmitted image (nonconfocal, scale bar corresponds to 10 μm) and confocal fluorescence images of pancreatic acinar cells before ($t=0$ s) and after ($t=2250$ s) stimulation with 20 μM POAEE. **(C)** The traces show the average time course with corresponding SEM error bars of ROS production in unstimulated cells in the absence (*gray*, $n=22$) or in the presence (*black*, $n=14$) of 5 μM rotenone and 10 μM antimycin. Note that the normalized fluorescence axis (F/F_0) on this figure is considerably expanded in comparison with the other figures shown in this article. *Right panel* shows transmitted image (nonconfocal, scale bar corresponds to 10 μm) and confocal fluorescence images of pancreatic acinar cells before ($t=450$ s) and after ($t=2250$ s) the application of rotenone and antimycin (note that in this case, the brightness of the fluorescence image did not change substantially). ACh, acetylcholine; POAEE, palmitoleic acid ethyl ester.

other cytotoxins from *P. aeruginosa* (37), the effects of pyocyanin on pancreatic acinar cells have not been described. Using our H_2RB-C_{18} dye, we observed substantial generation of ROS in response to 50 μM of pyocyanin (Fig. 5A). Pyocyanin also triggered $[Ca^{2+}]_i$ oscillations (Fig. 5B), mitochondrial depolarization, and transient increases in mitochondrial NAD(P)H (Fig. 5C). The pyocyanin-induced ROS production had two components—an initial rapid rise followed by a slow increase (Fig. 5D). The initial rapid rise was largely suppressed by blocking the mitochondrial electron transport chain (ETC) by rotenone (5 μM) plus antimycin (10 μM) (compare Fig. 5D, E). The slow rise, however, was observed in the presence of the ETC inhibitors (Fig. 5E). Therefore, the experiments with rotenone and antimycin revealed ETC-dependent (the major contributor to the initial rapid rise) and ETC-independent (the slow but resolvable increase of fluorescence) components of the response to pyocyanin. Mitochondria-targeted antioxidant MitoQ (34) effectively suppressed fluorescence changes induced by pyocyanin (Fig. 5F). The pyocyanin response was clearly observed in pancreatic acinar cells from *Ppif*$^{-/-}$ animals, suggesting that mitochondrial permeability transition (MPTP) is not essential for the pyocyanin response (Fig. 5G). The *Ppif* gene codes for cyclophilin D (peptidyl-prolyl isomerize

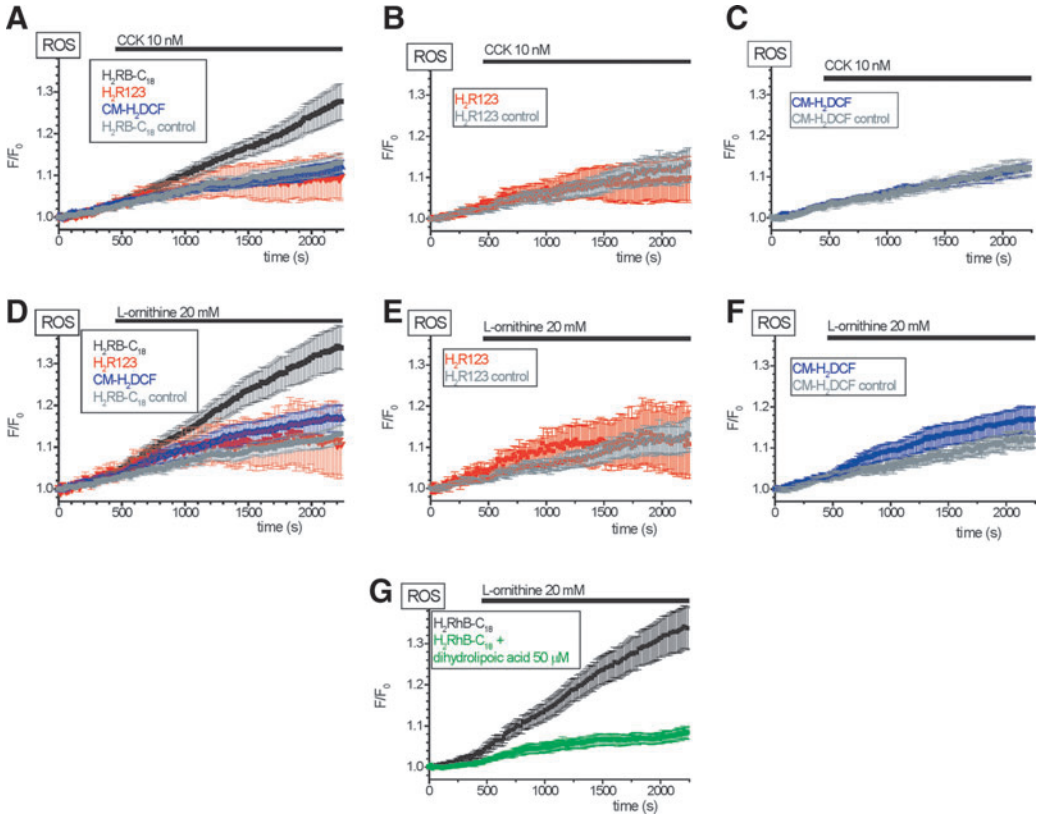

FIG. 4. Measuring ROS production with H_2RB-C_{18} and other probes. **(A)** Illustrates comparative sensitivity of H_2RB-C_{18} ($n=19$), H_2R123 ($n=24$), and CM-H_2DCF ($n=72$) in cells stimulated with CCK. Here and in parts **(B–G)**, the traces show the average time course of normalized fluorescence with the corresponding SEM error bars. The *gray trace* represents H_2RB-C_{18}-loaded control cells (cells that were not stimulated with CCK, $n=22$). Here and in **(D)**, the control traces for cells loaded with H_2R123 and CM-H_2DCF are not shown to avoid overloading the graph (the fluorescence of cells loaded with H_2R123 or CM-H_2DCF was not significantly different in the presence or absence of CCK). The fluorescence of CCK-treated cells loaded with H_2RB-C_{18} became statistically different from that recorded from the control cells after 560 s of stimulation. **(B)** Shows normalized fluorescence of cells loaded with H_2R123 and stimulated with CCK [*red trace*, $n=24$, the same trace as in **(A)**]. The *gray trace* represents H_2R123-loaded cells that were not stimulated with CCK ($n=29$). The fluorescence of cells loaded with H_2R123 was not significantly different in the presence or absence of CCK. **(C)** Shows normalized fluorescence of cells loaded with CM-H_2DCF and stimulated with CCK [*blue trace*, $n=24$, the same trace as in **(A)**]. The *gray trace* represents CM-H_2DCF-loaded cells that were not stimulated with CCK ($n=29$). The fluorescence of cells loaded with H_2R123 was not significantly different in the presence or absence of CCK. **(D)** Illustrates comparative sensitivities of H_2RB-C_{18} ($n=32$), H_2R123 ($n=11$), and CM-H_2DCF ($n=23$) in cells stimulated with L-ornithine (for more detailed analyses of L-ornithine response, see Fig. 5). **(E)** Shows normalized fluorescence of cells loaded with H_2R123 and stimulated with L-ornithine [*red trace*, $n=11$, the same trace as in **(D)**]. The *gray trace* represents H_2R123-loaded cells that were not stimulated with L-ornithine ($n=14$). **(F)** Shows normalized fluorescence of cells loaded with CM-H_2DCF and stimulated with L-ornithine [*blue trace*, $n=23$, the same trace as in **(D)**]. The *gray trace* represents CM-H_2DCF-loaded cells that were not stimulated with L-ornithine ($n=14$). **(G)** The fluorescence changes induced by L-ornithine in cells loaded with H_2RB-C_{18} in the presence of dihydrolipoic acid. The *black trace* [$n=32$, the same as in **(A)** and **(D)**] represents cells that were not treated by dihydrolipoic acid. The *green trace* represents cells that were pretreated with dihydrolipoic acid and stimulated with L-ornithine with the continuous presence of dihydrolipoic acid ($n=9$). CCK, cholecystokinin; H_2R123, dihydrorhodamine123; CM-H_2DCF, 5-(and-6)-chloromethyl-2′,7′-dichlorodihydrofluorescein.

known to regulate opening of the MPTP). These data indicate that pyocyanin induces significant ROS responses accompanied by prominent changes in NAD(P)H and $\Delta\Psi$.

Characterizing ROS responses induced by L-ornithine

In this part of the study, we used the H_2RB-C_{18} probe to detect the ROS changes induced by basic amino acids. Basic amino acids, at doses of a few grams per kilogram body weight, trigger AP in rodents (8, 23, 46, 53). Recently, it was suggested that L-arginine, which is most often used in these animal models of AP, may act through another basic amino acid L-ornithine (53). Using H_2RB-C_{18} dye, we detected ROS production induced by 20 m*M* L-ornithine (Fig. 6A, D), which is close to the dose of this amino acid used in the rat model of AP (53). L-ornithine also caused transient elevation of $[Ca^{2+}]_i$ (Fig. 6B) in a substantial proportion of tested cells (26/74). Other types of $[Ca^{2+}]_i$ responses to L-ornithine included (Supplementary Fig. S5) short spikes (5/74) and sustained elevations (35/74). Finally, 8 of the 74 cells did not display any $[Ca^{2+}]_i$ changes upon L-ornithine application. L-ornithine also caused mitochondrial depolarization

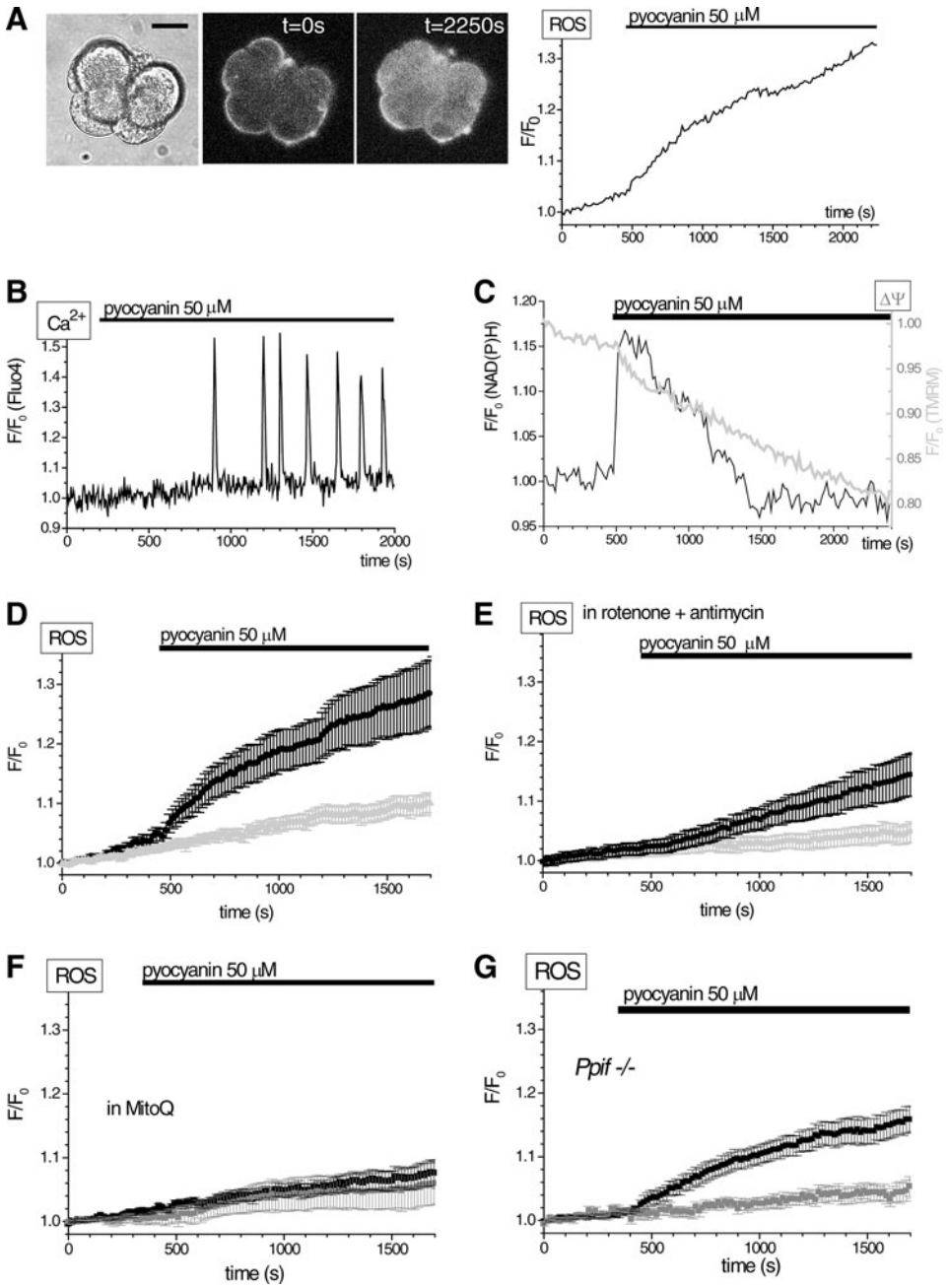

FIG. 5. ROS, $[Ca^{2+}]_i$, NAD(P)H, and ΔΨ responses to pyocyanin. **(A)** *Left panel* shows transmitted image (non-confocal, scale bar corresponds to 10 μm) and confocal fluorescence images of cells loaded with H_2RB-C_{18} before ($t = 0$ s) and after ($t = 2250$ s) stimulation with pyocyanin. *Right panel* shows pyocyanin-induced changes in normalized fluorescence in this group of cells. **(B)** An example of a $[Ca^{2+}]_i$ response (normalized Fluo-4 fluorescence) induced by pyocyanin (representative of 10 experiments). **(C)** NAD(P)H (*black*, left axis) and ΔΨ (TMRM fluorescence, *gray*, right axis) responses to pyocyanin. A decrease in TMRM fluorescence (the trace is representative of 19 experiments) corresponds to a decrease in ΔΨ (the trace is representative of 13 experiments). **(D)** ROS response to pyocyanin. The traces show fluorescence of cells stimulated with pyocyanin (*black*, $n = 12$) and of unstimulated cells (control, *gray*, $n = 22$) with the corresponding SEM error bars [here and in parts **(E–G)** cells were loaded with H_2RB-C_{18}]. The fluorescence of pyocyanin-treated cells became statistically different from that recorded from control cells after 20 s of stimulation. **(E)** ROS responses to pyocyanin in cells with inhibited mitochondrial respiratory chain. The traces show fluorescence of cells stimulated with pyocyanin (*black*, $n = 23$) and of unstimulated cells (control, *gray*, $n = 14$) with the corresponding SEM error bars; both stimulated and unstimulated cells (control) in these experiments were incubated in a solution containing rotenone (5 μM) and antimycin (10 μM). **(F)** MitoQ inhibits the fluorescence response of H_2RB-C_{18}-loaded cells to pyocyanin. The traces show fluorescence of cells stimulated with pyocyanin (*black*, $n = 7$) and of unstimulated cells (control, *gray*, $n = 8$) with the corresponding SEM error bars; both stimulated and unstimulated cells (control) in these experiments were incubated in a solution containing 1 μM MitoQ. **(G)** ROS response to pyocyanin in pancreatic acinar cells from *Ppif*$^{-/-}$ mice. The traces show fluorescence of cells stimulated with pyocyanin (*black*, $n = 24$) and of unstimulated cells (control, *gray*, $n = 10$) with the corresponding SEM error bars. TMRM, tetramethylrhodamine, methyl ester.

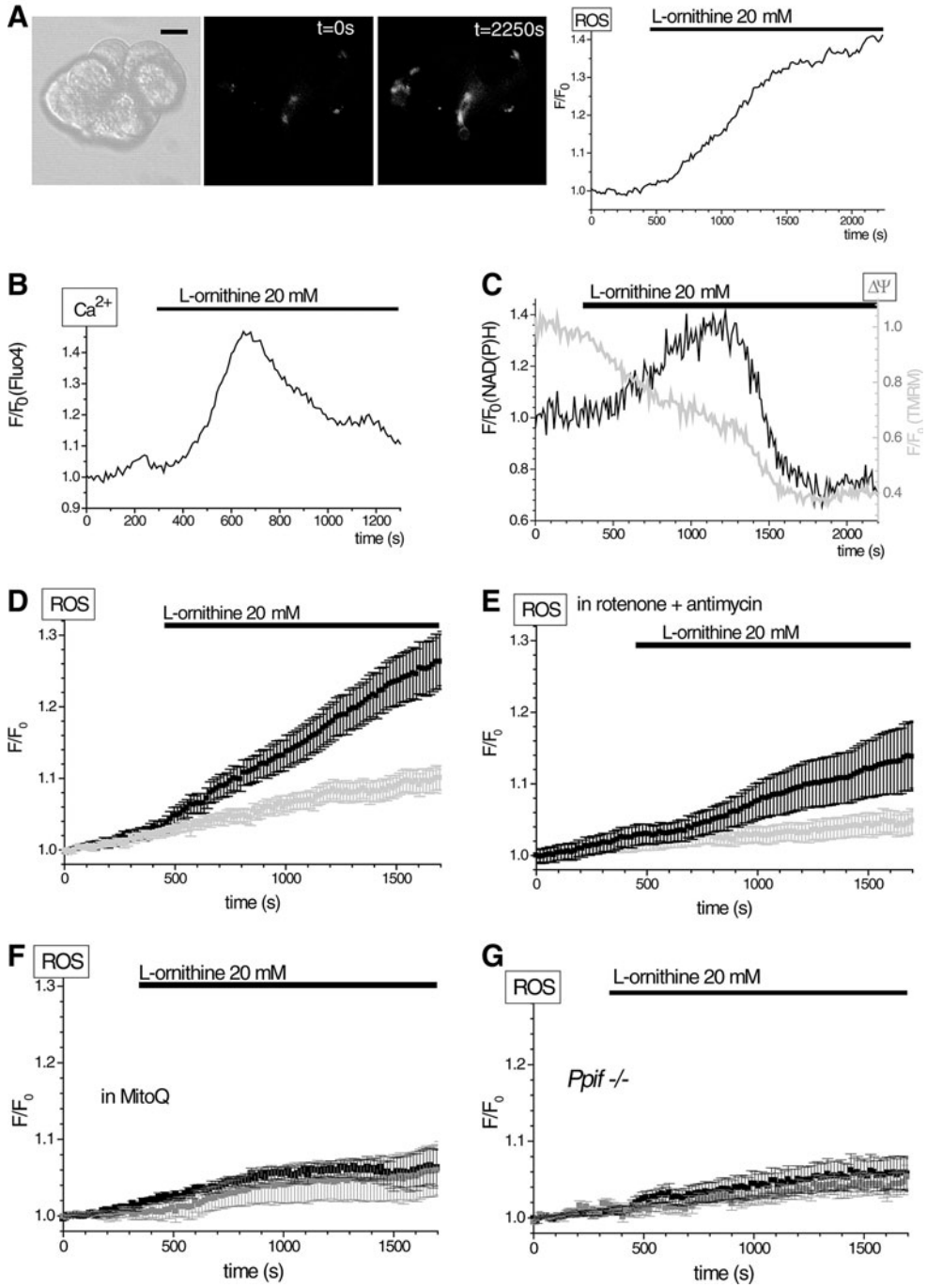

FIG. 6. ROS, $[Ca^{2+}]_i$, NAD(P)H, and ΔΨ responses to L-ornithine. **(A)** *Left panel* shows transmitted image (non-confocal, scale bar corresponds to 10 μm) and confocal fluorescence images of cells loaded with H_2RB-C_{18} before ($t = 0$ s) and after ($t = 2250$ s) stimulation with L-ornithine. *Right panel* shows L-ornithine-induced changes in normalized fluorescence in this group of cells. **(B)** An example of a $[Ca^{2+}]_i$ response (normalized fluorescence of Fluo-4) induced by L-ornithine. **(C)** NAD(P)H (*black*, left axis) and ΔΨ (TMRM fluorescence, *gray*, right axis) responses to L-ornithine. A decrease of TMRM fluorescence corresponds (the trace is representative of 15 experiments) to a decrease in ΔΨ (the trace is representative of 18 experiments). **(D)** ROS response to L-ornithine. Here and in **(E),** cells were loaded with H_2RB-C_{18}. The traces show normalized fluorescence of cells stimulated with L-ornithine (*black*, $n = 32$) and of unstimulated cells (control, *gray*, $n = 22$) with the corresponding SEM error bars. The fluorescence of L-onithine-treated cells became statistically different from that recorded from control cells after 200 s of stimulation. **(E)** ROS responses to L-ornithine in cells with an inhibited mitochondrial respiratory chain. The traces show fluorescence of cells stimulated with L-ornithine (*black*, $n = 30$) and of unstimulated cells (control, *gray*, $n = 14$) with the corresponding SEM error bars; both stimulated and unstimulated cells (control) in these experiments were incubated in a solution containing rotenone (5 μM) and antimycin (10 μM). **(F)** MitoQ inhibits the fluorescence response of H_2RB-C_{18}-loaded cells to L-ornithine. The traces show fluorescence of cells stimulated with L-ornithine (*black*, $n = 7$) and of unstimulated cells (control, *gray*, $n = 8$) with the corresponding SEM error bars; both stimulated and unstimulated cells (control) in these experiments were incubated in a solution containing MitoQ. **(G)** Illustrates the absence of fluorescence response to L-ornithine in pancreatic acinar cells from *Ppif*$^{-/-}$ mice. The traces show fluorescence of cells stimulated with L-ornithine (*black*, $n = 17$) and of unstimulated cells (control, *gray*, $n = 10$) with the corresponding SEM error bars.

(Fig. 6C) and a transient increase in NAD(P)H levels (Fig. 6C). A significant proportion of the ROS response to L-ornithine was eliminated when cells were treated with rotenone and antimycin, suggesting that the ETC is important for the L-ornithine response (Fig. 6D, E). MitoQ effectively suppressed the H_2RB-C_{18} fluorescence changes induced by L-ornithine (Fig. 6F). The response to L-ornithine was also strongly inhibited in pancreatic acinar cells from *Ppif*$^{-/-}$ animals (Fig. 6G). These data show that L-ornithine can produce potentially harmful calcium and mitochondrial responses and that the L-ornithine-induced ROS response has significant mitochondria-dependent component. L-arginine [another inducer of AP (23, 46, 53)] produced equipotent ROS responses to those of L-ornithine, whereas L-citrulline was less active (compare Fig. 7A with B and C).

Calcium dependency of responses to pyocyanin and L-ornithine

Pretreatment of the acinar cells with 30 μM 1,2-Bis(2-aminophenoxy)ethane-N,N,N′,N′-tetraacetic acid tetrakis (acetoxymethyl ester) (BAPTA-AM) (for 30 min) had a mild effect on the H_2RB-C_{18} fluorescence response to pyocyanin (not statistically significant for the majority of time points, see Fig. 8A), indicating that the rise in $[Ca^{2+}]_i$ is unlikely to be essential for the ROS response induced by pyocyanin. However, the pretreatment of the acinar cells with 30 μM BAPTA-AM (for 30 min) significantly suppressed the L-ornithine-induced ROS response (Fig. 8B), suggesting that in this case the ROS production requires $[Ca^{2+}]_i$ increase. Interestingly, the removal of Ca^{2+} from the extracellular solution also suppressed the H_2RB-C_{18} fluorescence response to L-ornithine (Fig. 8B), confirming the notion that Ca^{2+} signaling is important for this type of ROS response.

Discussion

The main technical advance in this study was the introduction of a new lipophilic ROS indicator, which preferentially reports ROS at membrane regions (and particularly the plasma membrane). The main findings were demonstration of pyocyanin-induced ROS production and characterization of ROS responses induced by the basic amino acids L-ornithine and L-arginine.

Difficulties in measuring ROS and reactive nitrogen species production in live cells using fluorescent probes are compounded by water-soluble antioxidants, such as glutathione and ascorbate, present in the cytoplasm in millimolar quantities. The membrane fraction contains alternative antioxidant system (2, 58). The relative efficiency of the cytosolic and membranous antioxidant systems is difficult to assess, but we hypothesize that the slower diffusion of antioxidants in membranes could make the integrative ROS probes (like reduced fluorescein and rhodamine derivatives) more sensitive if these could be targeted to the membrane compartments. We also considered that the membrane-localized probe will diffuse slower than water-soluble ROS sensors (and therefore could highlight the specific regions of ROS production). The indicator H_2RB-C_{18}, introduced in this study, is targeted to membrane compartments by its lipophilic C_{18} tail. The ability of molecules containing long lipophilic tails to flip in the plasma membrane and to translocate into internal membranes is determined by the properties of the

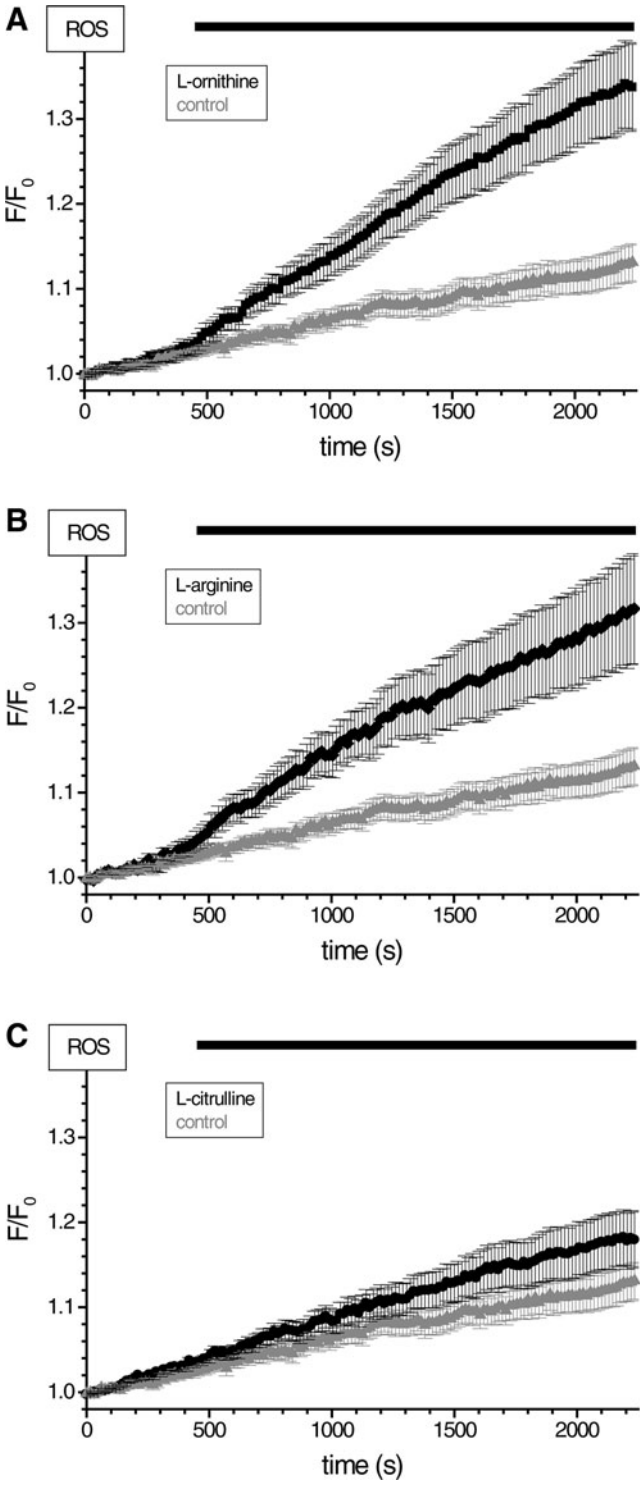

FIG. 7. Comparison of ROS responses to L-ornithine, L-arginine, and L-citrulline. Cells were loaded with H_2RB-C_{18}. The traces represent the averaged normalized fluorescence with corresponding SEM error bars. **(A)** The *black trace* represents ROS changes induced by 20 mM L-ornithine ($n = 32$). Normalized fluorescence of control (unstimulated) cells is shown by the *gray trace* [$n = 22$, the same ''control'' trace is shown in **(B)** and **(C)**]. **(B)** The *black trace* shows the ROS response to 20 mM L-arginine ($n = 10$). **(C)** The *black trace* shows the normalized H_2RB-C_{18} fluorescence in the presence of 20 mM L-citrulline ($n = 28$).

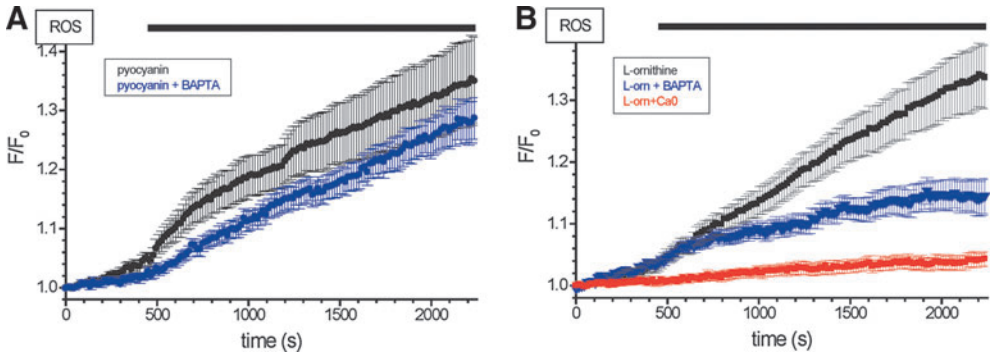

FIG. 8. ROS response to L-ornithine: effects of intracellular BAPTA and removal of extracellular Ca^{2+}. Cells were loaded with H_2RB-C_{18}. The traces represent the averaged normalized fluorescence with corresponding SEM error bars. **(A)** ROS changes in intact cells stimulated with 50 μM pyocyanin (*black*, $n=12$) or in cells preloaded with BAPTA (*blue*, $n=7$) by incubation for 30 min in a solution containing 30 μM BAPTA-AM and then stimulated with pyocyanin. **(B)** ROS changes in cells stimulated with 20 mM L-ornithine with no pretreatment (*black*, $n=32$) or in cells preloaded with BAPTA (*blue*, $n=17$) by incubation for 30 min in a solution containing 30 μM BAPTA-AM. The normalized H_2RB-C_{18} fluorescence of cells maintained in a Ca^{2+}-free extracellular solution (from the beginning of the experiment) and stimulated with 20 mM L-ornithine is shown by the *red trace* ($n=13$). BAPTA-AM, 1,2-Bis(2-aminophenoxy)ethane-N,N,N′,N′-tetraacetic acid tetrakis (acetoxymethyl ester).

part attached to the tail. For example, FIP-18 (lipophilic analogue of Ca^{2+} indicator Indo 1) effectively stains intracellular membranes, while Calcium Green C-18 stains plasma membrane and does not flip (11). The H_2RB is expected to be electrically neutral and therefore should not impede flipping and intracellular localization of the sensory part of the probe. Unlike other known lipophilic redox probes [such as BODIPY-based lipid peroxidation sensors (2)], it also benefits from the superior dynamic range common to ROS probes from the dihydrorhodamine family (which increase the quantum yield upon oxidation by two orders of magnitude). In conditions of our experiments, H_2RB-C_{18} showed better sensitivity to ROS in a cellular environment than the popular cytosolic ROS indicator H_2CMDCF, in response to at least two stimuli: 10 nM CCK and 20 mM L-ornithine. Furthermore, it also produced larger responses to stimulation with TLC-S. We assume that this increased sensitivity is due to reduced competition of the probe with antioxidants in the membrane compartments. Importantly, the C_{18} tail slows the diffusion of the probe and enables region-specific detection of ROS, which so far can only be achieved with targeted fluorescent proteins. Similar to CM-H_2DCF and H_2R123 (71), H_2RB-C_{18} does not react directly with superoxide radical and H_2O_2 but is effectively oxidized by products of the Fenton reaction (*i.e.,* probably to hydroxyl radical). It is likely that, similar to other dihydrorhodamines, H_2RB-C_{18} cannot specifically distinguish different types of ROS (22), as some proteins are able to do (4). However, the dynamic range of H_2RB-C_{18} is much greater than that seen in redox-sensitive proteins (54). Thus, we considered that H_2RB-C_{18} could be a useful tool in ROS research and proceeded to test this notion using primary isolated cells.

We applied H_2RB-C_{18} to detect ROS production in pancreatic acinar cells challenged by high doses of secretagogues and by other molecules implicated in pancreatic pathology (all these substances have been shown to trigger cytosolic Ca^{2+} responses). We resolved ROS responses to all tested substances. Most of the stimuli generated region-specific patterns of ROS changes. The highest signals were seen in the areas that had already shown the brightest fluorescence at the time the cells were first imaged (*i.e.,* before stimulation). These areas were usually located at the cell periphery in both apical and basal regions. However, some fluorescence changes were also recorded in the internal regions. The distribution of the fluorescence changes probably reflects both accumulation of the probe in the different cellular membranes (*e.g.,* plasma membrane and membranes of endoplasmic reticulum (ER) and the distribution of ROS sources. Among these putative ROS sources are subplasmalemmal mitochondria (49). This is a prominent group of mitochondria in pancreatic acinar cells, which are located in the immediate proximity of the plasma membrane (25, 49, 70), are juxtaposed in the junctions between the ER and the plasma membrane (43), and preferentially respond to the Ca^{2+} influx (49). We cannot exclude a possible contribution of NADPH oxidases, reported to be expressed in a pancreatic cell line (74) to the observed ROS responses; however, this enzyme could not be detected by immunohistochemistry (28) and did not participate in bile acid-induced ROS generation (15) in primary pancreatic acinar cells.

Large and fast fluorescence changes of our new probe were observed following the application of the *P. aeruginosa* toxin pyocyanin. This was the first study testing the effect of pyocyanin on ROS production, cell signaling, and mitochondria status of pancreatic acinar cells. Pancreatic infection with *P. aeruginosa* is a problem for AP, cystic fibrosis, and pancreatic transplantation or endoscopic retrograde cholangiopancreatography receiving patients (9, 13, 26, 42). The ability of pyocyanin to trigger substantial ROS changes, induce $[Ca^{2+}]_i$ and NAD(P)H responses, as well as its ability to reduce $\Delta\Psi$ (*i.e.,* to depolarize mitochondria and reduce the proton motive force vital for ATP production) suggests that this molecule can play an important role in the damage that *P. aeruginosa* causes in the pancreas and potentially in other organs. It is important to note that the decrease of tetramethylrhodamine, methyl ester (TMRM) fluorescence (*i.e.,* dissipation of $\Delta\Psi$) in experiments with pyocyanin was slow and NAD(P)H concentration during the initial fast phase of ROS production actually increased. These changes are clearly permissive for accelerated ROS production (Fig. 4) (61). The later decrease in the rate of ROS production could be partially attributed to

further loss of $\Delta\Psi$ and a delayed reduction in NAD(P)H. The effect of pyocyanin was observed in *Ppif*$^{-/-}$ mice, was not inhibited by buffering of cytosolic Ca^{2+} with BAPTA, but was strongly suppressed by MitoQ. These results suggest a possible direct (*i.e.,* not Ca^{2+}- or MPTP-mediated) interaction of pyocyanin with the mitochondria of the acinar cells and consequent ROS production and detection by H_2RB-C_{18}. The observed distribution of the H_2RB-C_{18} fluorescence during pyocyanin application (increase in the plasma membrane region) was clearly different from the distribution of mitochondria in pancreatic acinar cells, reported by a number of laboratories (25, 36, 49, 60, 64, 70). However, one group of mitochondria–subplasmalemmal mitochondria seems to be strategically positioned to mediate the observed response to pyocyanin. The role of these mitochondria will be investigated in a separate study.

We next applied H_2RB-C_{18} to investigate the responses induced by basic amino acids. L-ornithine generated clearly resolvable ROS responses (in addition to triggering $[Ca^{2+}]_i$, NADH, and $\Delta\Psi$ changes). L-arginine produced similar ROS responses, whereas L-citrulline was less effective. Interestingly, this correlates well with the reported potencies of AP induction by these amino acids in rats (53). The ROS response to L-ornithine appears to be dependent on $[Ca^{2+}]_i$ changes (or at least require some ''permissive'' $[Ca^{2+}]_i$), as the pretreatment of cells with the Ca^{2+}chelator BAPTA abolished the increase in H_2RB-C_{18} fluorescence. Strong inhibition of ROS response to L-ornithine by the removal of the extracellular Ca^{2+} is consistent with this conclusion. The importance of mitochondria for the L-ornithine-induced ROS response was highlighted by the inhibitory effects of MitoQ and by the significant decrease of L-ornithine response in *Ppif*$^{-/-}$ mice. A possible mechanism of the L-ornithine response could involve Ca^{2+} release from the internal stores, activation of the Ca^{2+} influx through the store-operated Ca^{2+} influx channels and Ca^{2+}-dependent (and possibly MPTP-dependent) acceleration of the mitochondrial ROS production. The importance of mitochondria for the ROS response observed in our study is consistent with a direct action of basic amino acids on the mitochondria of pancreatic acinar cells described recently (8).

Materials and Methods

Cell preparation, solutions, and chemicals

Pancreata were obtained from adult male mice (CD1), humanely killed in accordance with the Animals (Scientific Procedures) Act, 1986. The pancreatic acinar cells were isolated by digestion with purified collagenase (200 U/ml) as described previously (19) and used within 4 h.

Cyclophilin D-deficient mice generated by targeted disruption of the *Ppif* gene (3) were kindly provided by Dr. Derek Yellon (University College, London, United Kingdom).

The standard (for our laboratory) extracellular solution contained (in m*M*): NaCl, 140; KCl, 4.7; $MgCl_2$, 1.13; $CaCl_2$, 1.2; glucose, 10; HEPES-NaOH, 10 (pH 7.3). All the experiments were performed under continuous superfusion by the standard solution (controls) or by solutions based on this standard solution with the specified changes/additions. In amino acid-containing solutions, the NaCl concentration was decreased appropriately to maintain the osmolarity.

RB-C_{18} and all other chemicals, unless stated otherwise, were from Sigma-Aldrich. Fluo-4 acetoxymethyl ester (AM) and MitoTrackerRed were from Invitrogen, and collagenase was from Worthington Biomedical Corporation.

H_2RB-C_{18} preparation and dye loading

To produce the fluorogenic ROS probe, we added 10 μl of $NaBH_4$-containing solution (which was prepared as 1 mg/ml stock solution in DMSO) to 10 μl of DMSO-based solution containing 10 m*M* of RB-C_{18}. Within seconds, the mixture lost its red color, indicating the conversion of RB-C_{18} into H_2RB-C_{18}. Four microliters of glycerol and 16 μl of ethanol were then added to the mixture for 5 min to quench $NaBH_4$. H_2RB-C_{18} concentration in the stock solution (produced by the above-described procedure) was 2.5 m*M*. To load the pancreatic acinar cells, 40 μl of this H_2RB-C_{18}-containing stock solution was added immediately to a 10-ml suspension of freshly isolated acinar cells (the final concentration of H_2RB-C_{18} in the cell-containing solution was 10 μM) and incubated for 30 min at room temperature.

To study the responses of ROS sensors in cell-free system, 10 μM of the dyes dissolved in the extracellular buffer were tested by the addition of H_2O_2 (10 m*M*) followed by the addition of $CoCl_2$ (10 μM). The fluorescence and fluorescence spectra were recorded using the LS 50B spectrofluorometer (Perkin Elmer).

Cells were loaded with Fluo-4 by incubation in a solution containing 5 μM Fluo-4-AM for 30 min at room temperature. Cells were loaded with CM-H_2DCF by incubation in a solution containing 5 μM CM-H_2DCF(DA) for 30 min at 37°C. Cells were loaded with H_2R123 by incubation in a solution containing 5 μM of the probe for 30 min at 37°C. Cells were loaded with TMRM by incubation in a solution containing 50 n*M* TMRM for 30 min at 37°C.

Before the experiments, cells loaded with the fluorescent or fluorogenic probes were washed by centrifugation in a standard extracellular solution at room temperature.

Measurements of cell respiration

OCR of nonpermeabilized pancreatic acinar cells were assayed under basal and stress-test conditions using a Seahorse Bioscience XF24 Extracellular Flux Analyzer according to the manufacturer's specification (http://seahorsebio.com/products/consumables/kits/cell-mito-stress.php). In these experiments, cells were exposed to 10 μM H_2RB-C_{18} or 10 μM RB-C_{18}.

Imaging experiments and data analysis

Imaging experiments were performed at 28°C–30°C. Fluorescence images were obtained using Leica SP2 inverted confocal microscopes (Leica Microsystems). Cells loaded with H_2RB-C_{18} and TMRM were illuminated by 543 nm light using a $\times$63 1.2 NA objective lens. Low illumination laser power of 2%–3% and a fixed zoom factor (3.3) were used in all experiments with H_2RB-C_{18}. Fluorescence emission was recorded at 560–620 nm. The recordings started after a 5-min baseline settling period. Recordings of H_2RB-C_{18} fluorescence in unstimulated cells (control experiments) obtained throughout the duration of the project were pooled together, processed, and shown for comparison on appropriate figures.

Cells loaded with Fluo-4, CM-H_2DCF, and H_2R123 were illuminated by 496 nm light, and fluorescence of these probes was recorded at 520–560 nm. The fluorescence of NAD(P)H was excited using 365 nm laser line and recorded at 450–490 nm. The results of fluorescence measurements were presented as normalized data by dividing the raw data by the average value of the fluorescence recorded for the first five time points. Results are reported as mean ± SEM. Statistical comparisons were performed using the Student's *t*-test, and statistical significance was assumed at $p < 0.05$.

Acknowledgments

The work was supported by the Medical Research Council (UK) grants G0700167 and MR/K012967/1 and by the National Institute for Health Research (UK) grant to the NIHR Liverpool Pancreas Biomedical Research Unit. The assistance of Hayley Dingsdale, David Collier, and Svetlana Voronina is gratefully acknowledged.

Author Disclosure Statement

The authors declare that no competing financial interests exist.

References

1. Baggaley EM, Elliott AC, and Bruce JI. Oxidant-induced inhibition of the plasma membrane Ca2+-ATPase in pancreatic acinar cells: role of the mitochondria. *Am J Physiol Cell Physiol* 295: C1247–C1260, 2008.
2. Bain PA and Schuller KA. Use of fluorogenic probes to differentiate between hydrophilic and lipophilic antioxidant activity in a fish cell line. *J Agric Food Chem* 60: 699–705, 2012.
3. Baines CP, Kaiser RA, Purcell NH, Blair NS, Osinska H, Hambleton MA, Brunskill EW, Sayen MR, Gottlieb RA, Dorn GW, Robbins J, and Molkentin JD. Loss of cyclophilin D reveals a critical role for mitochondrial permeability transition in cell death. *Nature* 434: 658–662, 2005.
4. Belousov VV, Fradkov AF, Lukyanov KA, Staroverov DB, Shakhbazov KS, Terskikh AV, and Lukyanov S. Genetically encoded fluorescent indicator for intracellular hydrogen peroxide. *Nat Methods* 3: 281–286, 2006.
5. Bhardwaj P, Garg PK, Maulik SK, Saraya A, Tandon RK, and Acharya SK. A randomized controlled trial of antioxidant supplementation for pain relief in patients with chronic pancreatitis. *Gastroenterology* 136: 149–159, 2009.
6. Bhatia M. Apoptosis versus necrosis in acute pancreatitis. *Am J Physiol Gastrointest Liver Physiol* 286: G189–G196, 2004.
7. Bhogal RH, Curbishley SM, Weston CJ, Adams DH, and Afford SC. Reactive oxygen species mediate human hepatocyte injury during hypoxia/reoxygenation. *Liver Transpl* 16: 1303–1313, 2010.
8. Biczo G, Hegyi P, Dosa S, Shalbuyeva N, Berczi S, Sinervirta R, Hracsko Z, Siska A, Kukor Z, Jarmay K, Venglovecz V, Varga IS, Ivanyi B, Alhonen L, Wittmann T, Gukovskaya A, Takacs T, and Rakonczay Z, Jr. The crucial role of early mitochondrial injury in L-lysine-induced acute pancreatitis. *Antioxid Redox Signal* 15: 2669–2681, 2011.
9. Biggar WD, Holmes B, and Good RA. Opsonic defect in patients with cystic fibrosis of the pancreas. *Proc Natl Acad Sci U S A* 68: 1716–1719, 1971.
10. Biwersi J and Verkman AS. Cell-permeable fluorescent indicator for cytosolic chloride. *Biochemistry* 30: 7879–7883, 1991.
11. Blatter LA and Niggli E. Confocal near-membrane detection of calcium in cardiac myocytes. *Cell Calcium* 23: 269–279, 1998.
12. Bogeski I, Kummerow C, Al-Ansary D, Schwarz EC, Koehler R, Kozai D, Takahashi N, Peinelt C, Griesemer D, Bozem M, Mori Y, Hoth M, and Niemeyer BA. Differential redox regulation of ORAI ion channels: a mechanism to tune cellular calcium signaling. *Sci Signal* 3: ra24, 2010.
13. Bonatti H, Steurer W, Konigsrainer A, Allerberger F, and Margreiter R. Infection of the pancreatic duct following pancreas transplantation with bladder drainage. *J Chemother* 7: 442–445, 1995.
14. Booth DM, Mukherjee R, Sutton R, and Criddle DN. Calcium and reactive oxygen species in acute pancreatitis: friend or foe? *Antioxid Redox Signal* 15: 2683–2698, 2011.
15. Booth DM, Murphy JA, Mukherjee R, Awais M, Neoptolemos JP, Gerasimenko OV, Tepikin AV, Petersen OH, Sutton R, and Criddle DN. Reactive oxygen species induced by bile acid induce apoptosis and protect against necrosis in pancreatic acinar cells. *Gastroenterology* 140: 2116–2125, 2011.
16. Boulton S, Anderson A, Swalwell H, Henderson JR, Manning P, and Birch-Machin MA. Implications of using the fluorescent probes, dihydrorhodamine 123 and 2′,7′-dichlorodihydrofluorescein diacetate, for the detection of UVA-induced reactive oxygen species. *Free Radic Res* 45: 139–146, 2011.
17. Caldwell CC, Chen Y, Goetzmann HS, Hao Y, Borchers MT, Hassett DJ, Young LR, Mavrodi D, Thomashow L, and Lau GW. *Pseudomonas aeruginosa* exotoxin pyocyanin causes cystic fibrosis airway pathogenesis. *Am J Pathol* 175: 2473–2488, 2009.
18. Camello C, Camello PJ, Pariente JA, and Salido GM. Effects of antioxidants on calcium signal induced by cholecystokinin in mouse pancreatic acinar cells. *J Physiol Biochem* 56: 173–180, 2000.
19. Chvanov M, Gerasimenko OV, Petersen OH, and Tepikin AV. Calcium-dependent release of NO from intracellular S-nitrosothiols. *EMBO J* 25: 3024–3032, 2006.
20. Chvanov M, Petersen OH, and Tepikin A. Free radicals and the pancreatic acinar cells: role in physiology and pathology. *Philos Trans R Soc Lond B Biol Sci* 360: 2273–2284, 2005.
21. Criddle DN, Gillies S, Baumgartner-Wilson HK, Jaffar M, Chinje EC, Passmore S, Chvanov M, Barrow S, Gerasimenko OV, Tepikin AV, Sutton R, and Petersen OH. Menadione-induced reactive oxygen species generation via redox cycling promotes apoptosis of murine pancreatic acinar cells. *J Biol Chem* 281: 40485–40492, 2006.
22. Crow JP. Dichlorodihydrofluorescein and dihydrorhodamine 123 are sensitive indicators of peroxynitrite *in vitro*: implications for intracellular measurement of reactive nitrogen and oxygen species. *Nitric Oxide* 1: 145–157, 1997.
23. Dawra R, Sharif R, Phillips P, Dudeja V, Dhaulakhandi D, and Saluja AK. Development of a new mouse model of acute pancreatitis induced by administration of L-arginine. *Am J Physiol Gastrointest Liver Physiol* 292: G1009–G1018, 2007.
24. Dickinson BC and Chang CJ. Chemistry and biology of reactive oxygen species in signaling or stress responses. *Nat Chem Biol* 7: 504–511, 2011.

25. Dolman NJ, Gerasimenko JV, Gerasimenko OV, Voronina SG, Petersen OH, and Tepikin AV. Stable Golgi-mitochondria complexes and formation of Golgi Ca(2+) gradients in pancreatic acinar cells. *J Biol Chem* 280: 15794–15799, 2005.
26. Garg PK, Khanna S, Bohidar NP, Kapil A, and Tandon RK. Incidence, spectrum and antibiotic sensitivity pattern of bacterial infections among patients with acute pancreatitis. *J Gastroenterol Hepatol* 16: 1055–1059, 2001.
27. Grady T, Saluja A, Kaiser A, and Steer M. Edema and intrapancreatic trypsinogen activation precede glutathione depletion during caerulein pancreatitis. *Am J Physiol* 271: G20–G26, 1996.
28. Gukovskaya AS, Perkins P, Zaninovic V, Sandoval D, Rutherford R, Fitzsimmons T, Pandol SJ, and Poucell-Hatton S. Mechanisms of cell death after pancreatic duct obstruction in the opossum and the rat. *Gastroenterology* 110: 875–884, 1996.
29. Harper ME, Bevilacqua L, Hagopian K, Weindruch R, and Ramsey JJ. Ageing, oxidative stress, and mitochondrial uncoupling. *Acta Physiol Scand* 182: 321–331, 2004.
30. Iborra M, Moret I, Rausell F, Bastida G, Aguas M, Cerrillo E, Nos P, and Beltran B. Role of oxidative stress and antioxidant enzymes in Crohn's disease. *Biochem Soc Trans* 39: 1102–1106, 2011.
31. Jaeschke H. Reactive oxygen and mechanisms of inflammatory liver injury: present concepts. *J Gastroenterol Hepatol* 26 Suppl 1: 173–179, 2011.
32. Jakubowski W and Bartosz G. 2,7-dichlorofluorescin oxidation and reactive oxygen species: what does it measure? *Cell Biol Int* 24: 757–760, 2000.
33. Kaiser AM, Saluja AK, Sengupta A, Saluja M, and Steer ML. Relationship between severity, necrosis, and apoptosis in five models of experimental acute pancreatitis. *Am J Physiol* 269: C1295–C1304, 1995.
34. Kelso GF, Porteous CM, Coulter CV, Hughes G, Porteous WK, Ledgerwood EC, Smith RA, and Murphy MP. Selective targeting of a redox-active ubiquinone to mitochondria within cells: antioxidant and antiapoptotic properties. *J Biol Chem* 276: 4588–4596, 2001.
35. Kiani-Esfahani A, Tavalaee M, Deemeh MR, Hamiditabar M, and Nasr-Esfahani MH. DHR123: an alternative probe for assessment of ROS in human spermatozoa. *Syst Biol Reprod Med* 58: 168–174, 2012.
36. Kidd JF, Pilkington MF, Schell MJ, Fogarty KE, Skepper JN, Taylor CW, and Thorn P. Paclitaxel affects cytosolic calcium signals by opening the mitochondrial permeability transition pore. *J Biol Chem* 277: 6504–6510, 2002.
37. Lau PP, Palmer RL, Lambert HC, Song CS, Lutz F, and Geokas MC. *Pseudomonas aeruginosa* cytotoxin stimulates secretion of amylase and protease zymogens with a concomitant decrease of mRNA levels in isolated rat pancreatic acini. *Biochem Biophys Res Commun* 152: 688–694, 1988.
38. LeBel CP, Ischiropoulos H, and Bondy SC. Evaluation of the probe 2′,7′-dichlorofluorescin as an indicator of reactive oxygen species formation and oxidative stress. *Chem Res Toxicol* 5: 227–231, 1992.
39. Lerch MM and Gorelick FS. Models of acute and chronic pancreatitis. *Gastroenterology* 144: 1180–1193, 2013.
40. Leung PS and Chan YC. Role of oxidative stress in pancreatic inflammation. *Antioxid Redox Signal* 11: 135–165, 2009.
41. Loh KP, Huang SH, De SR, Tan BK, and Zhu YZ. Oxidative stress: apoptosis in neuronal injury. *Curr Alzheimer Res* 3: 327–337, 2006.
42. Low DE, Micflikier AB, Kennedy JK, and Stiver HG. Infectious complications of endoscopic retrograde cholangiopancreatography. A prospective assessment. *Arch Intern Med* 140: 1076–1077, 1980.
43. Lur G, Haynes LP, Prior IA, Gerasimenko OV, Feske S, Petersen OH, Burgoyne RD, and Tepikin AV. Ribosome-free terminals of rough ER allow formation of STIM1 puncta and segregation of STIM1 from IP(3) receptors. *Curr Biol* 19: 1648–1653, 2009.
44. Luthen R, Niederau C, and Grendell JH. Intrapancreatic zymogen activation and levels of ATP and glutathione during caerulein pancreatitis in rats. *Am J Physiol* 268: G592–G604, 1995.
45. Miesel R, Hartung R, and Kroeger H. Priming of NADPH oxidase by tumor necrosis factor alpha in patients with inflammatory and autoimmune rheumatic diseases. *Inflammation* 20: 427–438, 1996.
46. Mizunuma T, Kawamura S, and Kishino Y. Effects of injecting excess arginine on rat pancreas. *J Nutr* 114: 467–471, 1984.
47. Neuschwander-Tetri BA, Ferrell LD, Sukhabote RJ, and Grendell JH. Glutathione monoethyl ester ameliorates caerulein-induced pancreatitis in the mouse. *J Clin Invest* 89: 109–116, 1992.
48. Odinokova IV, Sung KF, Mareninova OA, Hermann K, Evtodienko Y, Andreyev A, Gukovsky I, and Gukovskaya AS. Mechanisms regulating cytochrome c release in pancreatic mitochondria. *Gut* 58: 431–442, 2009.
49. Park MK, Ashby MC, Erdemli G, Petersen OH, and Tepikin AV. Perinuclear, perigranular and sub-plasmalemmal mitochondria have distinct functions in the regulation of cellular calcium transport. *EMBO J* 20: 1863–1874, 2001.
50. Petersen OH, Gerasimenko OV, and Gerasimenko JV. Pathobiology of acute pancreatitis: focus on intracellular calcium and calmodulin. *F1000 Med Rep* 3: 15, 2011.
51. Petersen OH and Tepikin AV. Polarized calcium signaling in exocrine gland cells. *Annu Rev Physiol* 70: 273–299, 2008.
52. Petrov MS. Therapeutic implications of oxidative stress in acute and chronic pancreatitis. *Curr Opin Clin Nutr Metab Care* 13: 562–568, 2010.
53. Rakonczay Z, Jr., Hegyi P, Dosa S, Ivanyi B, Jarmay K, Biczo G, Hracsko Z, Varga IS, Karg E, Kaszaki J, Varro A, Lonovics J, Boros I, Gukovsky I, Gukovskaya AS, Pandol SJ, and Takacs T. A new severe acute necrotizing pancreatitis model induced by L-ornithine in rats. *Crit Care Med* 36: 2117–2127, 2008.
54. Rhee SG, Chang TS, Jeong W, and Kang D. Methods for detection and measurement of hydrogen peroxide inside and outside of cells. *Mol Cells* 29: 539–549, 2010.
55. Rodriguez J, Specian V, Maloney R, Jourd'heuil D, and Feelisch M. Performance of diamino fluorophores for the localization of sources and targets of nitric oxide. *Free Radic Biol Med* 38: 356–368, 2005.
56. Sah RP and Saluja A. Molecular mechanisms of pancreatic injury. *Curr Opin Gastroenterol* 27: 444–451, 2011.
57. Saluja A, Hofbauer B, Yamaguchi Y, Yamanaka K, and Steer M. Induction of apoptosis reduces the severity of caerulein-induced pancreatitis in mice. *Biochem Biophys Res Commun* 220: 875–878, 1996.

58. Sedlak TW, Saleh M, Higginson DS, Paul BD, Juluri KR, and Snyder SH. Bilirubin and glutathione have complementary antioxidant and cytoprotective roles. *Proc Natl Acad Sci U S A* 106: 5171–5176, 2009.
59. Siriwardena AK, Mason JM, Balachandra S, Bagul A, Galloway S, Formela L, Hardman JG, and Jamdar S. Randomised, double blind, placebo controlled trial of intravenous antioxidant (n-acetylcysteine, selenium, vitamin C) therapy in severe acute pancreatitis. *Gut* 56: 1439–1444, 2007.
60. Straub SV, Giovannucci DR, and Yule DI. Calcium wave propagation in pancreatic acinar cells: functional interaction of inositol 1,4,5-trisphosphate receptors, ryanodine receptors, and mitochondria. *J Gen Physiol* 116: 547–560, 2000.
61. Suski JM, Lebiedzinska M, Bonora M, Pinton P, Duszynski J, and Wieckowski MR. Relation between mitochondrial membrane potential and ROS formation. *Methods Mol Biol* 810: 183–205, 2012.
62. Sutton R, Petersen OH, and Pandol SJ. Pancreatitis and calcium signalling: report of an international workshop. *Pancreas* 36: e1–e14, 2008.
63. Thrower E, Husain S, and Gorelick F. Molecular basis for pancreatitis. *Curr Opin Gastroenterol* 24: 580–585, 2008.
64. Tinel H, Cancela JM, Mogami H, Gerasimenko JV, Gerasimenko OV, Tepikin AV, and Petersen OH. Active mitochondria surrounding the pancreatic acinar granule region prevent spreading of inositol trisphosphate-evoked local cytosolic Ca(2+) signals. *EMBO J* 18: 4999–5008, 1999.
65. Tolleshaug H. Fluorescent contrast agent. 11/721,346 [US2009/0238765A1], 7–13. 2007. USA. 13-12-2005.
66. Valko M, Izakovic M, Mazur M, Rhodes CJ, and Telser J. Role of oxygen radicals in DNA damage and cancer incidence. *Mol Cell Biochem* 266: 37–56, 2004.
67. van Westerloo DJ, Schultz MJ, Bruno MJ, de Vos AF, Florquin S, and van der Poll T. Acute pancreatitis in mice impairs bacterial clearance from the lungs, whereas concurrent pneumonia prolongs the course of pancreatitis. *Crit Care Med* 32: 1997–2001, 2004.
68. Verlaan M, Roelofs HM, van-Schaik A, Wanten GJ, Jansen JB, Peters WH, and Drenth JP. Assessment of oxidative stress in chronic pancreatitis patients. *World J Gastroenterol* 12: 5705–5710, 2006.
69. Voronina S, Sukhomlin T, Johnson PR, Erdemli G, Petersen OH, and Tepikin A. Correlation of NADH and Ca2+ signals in mouse pancreatic acinar cells. *J Physiol* 539: 41–52, 2002.
70. Voronina SG, Barrow SL, Gerasimenko OV, Petersen OH, and Tepikin AV. Effects of secretagogues and bile acids on mitochondrial membrane potential of pancreatic acinar cells: comparison of different modes of evaluating DeltaPsim. *J Biol Chem* 279: 27327–27338, 2004.
71. Wardman P. Fluorescent and luminescent probes for measurement of oxidative and nitrosative species in cells and tissues: progress, pitfalls, and prospects. *Free Radic Biol Med* 43: 995–1022, 2007.
72. Wilhelm J, Vytasek R, Ostadalova I, and Vajner L. Evaluation of different methods detecting intracellular generation of free radicals. *Mol Cell Biochem* 328: 167–176, 2009.
73. Wilson R, Sykes DA, Watson D, Rutman A, Taylor GW, and Cole PJ. Measurement of *Pseudomonas aeruginosa* phenazine pigments in sputum and assessment of their contribution to sputum sol toxicity for respiratory epithelium. *Infect Immun* 56: 2515–2517, 1988.
74. Yu JH, Lim JW, Kim H, and Kim KH. NADPH oxidase mediates interleukin-6 expression in cerulein-stimulated pancreatic acinar cells. *Int J Biochem Cell Biol* 37: 1458–1469, 2005.

Address correspondence to:
Dr. Alexei V. Tepikin
Department of Cellular and Molecular Physiology
Institute of Translational Medicine
The University of Liverpool
Crown St.
Liverpool L69 3BX
United Kingdom

E-mail: a.tepikin@liverpool.ac.uk

Date of first submission to ARS Central, August 23, 2013; date of final revised submission, February 25, 2014; date of acceptance, March 16, 2014.

Abbreviations Used

$\Delta\Psi$ = mitochondrial membrane potential
ACh = acetylcholine
AP = acute pancreatitis
BAPTA-AM = 1,2-Bis(2-aminophenoxy)ethane-N,N,N′,N′-tetraacetic acid tetrakis (acetoxymethyl ester)
CCK = cholecystokinin
CM-H_2DCF = 5-(and-6)-chloromethyl-2′,7′-dichlorodihydrofluorescein
CM-H_2DCF(DA) = 5-(and-6)-chloromethyl-2′,7′-dichlorodihydrofluorescein diacetate
DMSO = dimethyl sulfoxide
ER = endoplasmic reticulum
ETC = electron transport chain
FCCP = carbonyl cyanide 4-(trifluoromethoxy) phenylhydrazone
H_2O_2 = hydrogen peroxide
H_2R123 = dihydrorhodamine123
H_2RB-C_{18} = dihydrorhodamine B octadecyl ester
MPTP = mitochondrial permeability transition
$NaBH_4$ = sodium borohydride
OCR = oxygen consumption rate
POAEE = palmitoleic acid ethyl ester
R123 = rhodamine123
RB-C_{18} = rhodamine B octadecyl ester
ROS = reactive oxygen species
TLC-S = taurolithocholic acid 3-sulfate
TMRM = tetramethylrhodamine, methyl ester

This work is licensed under a Creative Commons Attribution 3.0 United States License. You are free to copy, distribute, transmit and adapt this work, but you must attribute this work as ''Antioxidants & Redox Signaling. Copyright 2014 Mary Ann Liebert, Inc. http://liebertpub.com/ars, used under a Creative Commons Attribution License: http://creativecommons.org/licenses/by/3.0/us/''